Astronomy
&
Astrophysics

Discovery of a dust cloud next to σ Orionis

J. Th. van Loon and J. M. Oliveira

Astrophysics Group, School of Chemistry & Physics, Keele University, Staffordshire ST5 5BG, UK

Abstract. We report on the discovery of a mid-infrared source at a projected distance of only 1200 AU from the O9.5 V star σ Orionis. The spatially resolved, fan-shaped morphology and the presence of an ionization front, as well as evidence in the spectrum for processed dust grains, all suggest that it is a proto-planetary disk being dispersed by the intense ultraviolet radiation from σ Orionis. We compute the mass budget and the photo-evaporation timescale, and discuss the possible nature of this remarkable object.

Key words. circumstellar matter – stars: formation – stars: individual: σ Orionis (HD 37468) – planetary systems: protoplanetary disks – infrared: stars

1. Introduction

1.1. Proto-planetary disks

The conservation of angular momentum in a collapsing and fragmenting molecular cloud naturally leads to the presence of circumstellar disks around young stellar objects. It is believed that by way of co-agulation of dust and subsequent accretion of gas planets may form in these disks – whence their name "proto-planetary disk".

The evolution of a proto-planetary disk into a planetary system must compete with a multitude of disk-dispersal mechanisms: accretion, stellar wind and photo-evaporation by the central star depletes the disk from the inside, whilst nearby hot, massive O- and B-type stars photo-evaporate the disk from the outside. Censuses of circumstellar disks in several young stellar clusters, though prone to observational bias, suggest that most disks disappear in ~6 Myr (Haisch et al. 2001).

Photo-evaporation of disks by external stars has been observed to happen in the Orion Nebula (O'Dell et al. 1993) and in the massive star forming region NGC 3603 (Brandner et al. 2000). In these harsh environments, the effect of the intense UV radiation is expected to disperse the disks on timescales of only ~10^5 yr, which is much quicker than the ages of the young clusters in the Orion Nebula (1–2 Myr: McCaughrean & Stauffer 1994) and NGC 3603 (3 Myr: Hofmann et al. 1995).

1.2. σ Orionis and the σ Orionis cluster

At a Hipparcos distance of 352 pc, the bright ($m_V = 3.8$ mag) O9.5 V star σ Orionis is the primary component of a quintuple system of O and B stars (ADS 4241). ADS 4241 AB sits at the heart of the most massive visual binary known, with estimated masses of $M_A \simeq 25\ M_\odot$ and $M_B \simeq 15\ M_\odot$, an orbital period $P = 158$ yr, semi-major axis $a = 0.265''$, eccentricity $e = 0.06$

and inclination $i = 153°$ (Heintz 1997). The early B-type companions C and D are much farther away, at projected distances of $d \simeq 11''$ to the West and $d \simeq 13''$ to the East, respectively. At $d \simeq 42''$ to the East-Northeast, the helium-rich B2 Vp star σ Ori E is the most remote companion.

This massive multiple system is part of the Orion OB1 association (Brown et al. 1994) and forms the core of a recently discovered (Walter et al. 1997) young cluster of stars, brown dwarfs and isolated planetary mass objects (Zapatero Osorio et al. 2000), with an age of ~4 Myr (Oliveira et al. 2002). Its immediate vicinity is largely free of dust and molecular material. This cluster is in a crucial phase in terms of disk dispersal, and we have obtained IR data (L- and N-band) to detect and characterize circumstellar disks around cluster members across the entire mass range (Oliveira et al. 2003).

One of the peculiarities of σ Orionis that so far has received little attention is its association with a bright source of mid-IR emission, IRAS 05362−0237. One might try to attribute it to free-free emission from the boundary between the colliding winds of ADS 4241 A and B, but this interpretation is not supported by the shape of the IR spectral energy distribution, and its X-ray luminosity is typical for the relatively weak stellar wind of σ Orionis with a mass-loss rate of $\dot{M} < 10^{-8}\ M_\odot\ \mathrm{yr}^{-1}$ (Chlebowski & Garmany 1991). Nevertheless, when radio emission was detected from a position 2–3$''$ to the North of σ Orionis it was again attributed to (probably non-thermal) emission from ADS 4241 AB, with the positional mismatch between the accurate radio position and the USNO optical position of σ Orionis deemed insignificant (Drake 1990).

2. Sub-arcsecond mid-IR observations of σ Orionis

The mid-IR imager and spectrograph TIMMI-2 at the ESO 3.6 m telescope at La Silla, Chile, was used on the night
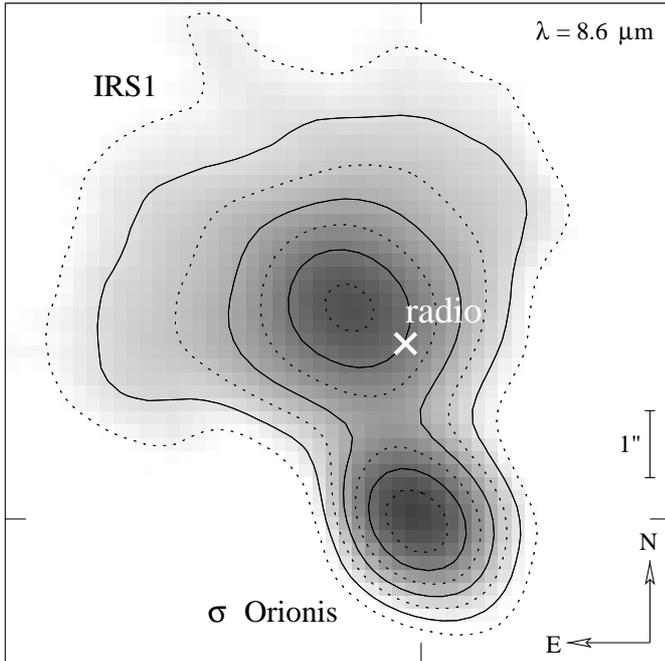
Fig. 1. Mid-infrared image of σ Orionis (near the bottom) and IRS1 (near the centre), taken through the $N1$-band ($\lambda_0 = 8.6\,\mu$m) filter with the TIMMI-2 camera at the ESO 3.6 m telescope. The position of the radio source as detected by Drake (1990) is indicated by a white cross. The field measures $10'' \times 10''$, with North up and East to the left, and is displayed on a logarithmic scale with a dynamic range of a factor 100.

Fig. 2. N-band spectra of σ Orionis (circles) and σ Ori IRS1 (dots). The spectrum of σ Orionis shows a pure photospheric continuum, but the spectrum of σ Ori IRS1 exhibits a strong, broad emission feature indicative of silicate dust.

of 15/16 December, 2002. Images of σ Orionis were obtained through the $N1$-band filter ($\lambda_0 = 8.6\,\mu$m, $\Delta\lambda = 1.2\,\mu$m for Full-Width at Half Maximum (*FWHM*) and $\Delta\lambda = 1.7\,\mu$m between blue and red cut-off) and through the $Q1$-band filter ($\lambda_0 = 17.75\,\mu$m, $\Delta\lambda = 0.8\,\mu$m for *FWHM* and $\Delta\lambda = 1.4\,\mu$m between blue and red cut-off). The pixel scale was $0.2''$ pixel^{-1}, resulting in a $64'' \times 48''$ (RA $\times$ Dec) field-of-view. We used a chop throw of $10''$ in the N-S direction and a nod offset of $10''$ in the E-W direction. The resulting stellar images had a *FWHM* of 0.7–$0.8''$. Photometry was performed on the shift-added images, using a circular software aperture with a $2''$ diameter, and calibrated against HD 4128 and HD 32887.

TIMMI-2 was used on the same night for spectroscopy. With a slit of $3''$ wide and $50''$ long, the spectral resolving power, limited by the pixel scale of $0.02\,\mu$m pixel^{-1}, was $R \sim 200$–300 across a useful window of $\lambda = 8$ to $13\,\mu$m. The spectrum was flux-calibrated against HD 4128 and HD 32887 as well as the $N1$-band photometry.

3. Discovery of σ Ori IRS1

3.1. Imagery

The discovery of *another* bright mid-IR source (Fig. 1) – which we designate σ Ori IRS1 – next to σ Orionis came totally unexpected. The new object has a compact core at only $3.3''$ to the North-Northeast from σ Orionis, and also exhibits extended emission in a fan-shaped morphology, pointing away from σ Orionis. The image in Fig. 1 was obtained after one iteration of a deconvolution algorithm (Lucy 1974) within the
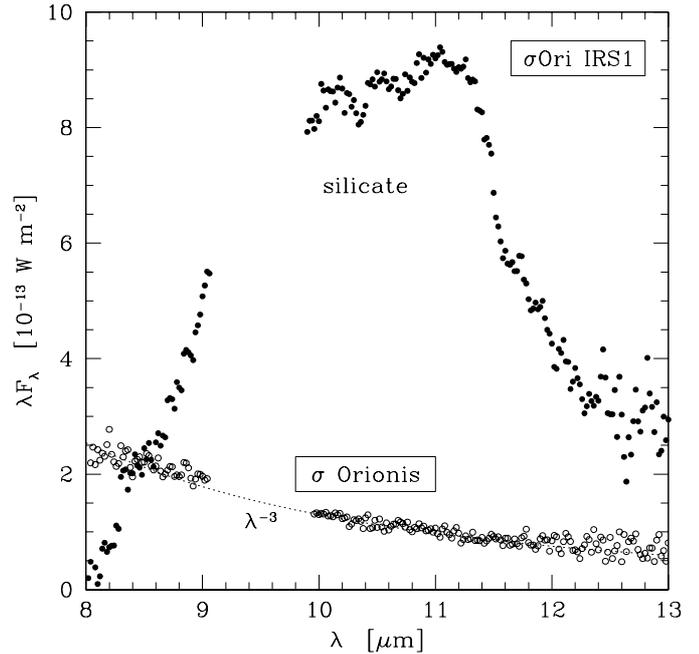
ESO software package MIDAS, using σ Orionis as a model for the Point Spread Function.

The close proximity of IRS1 to the mag 4 star σ Orionis is the main reason why this object has so far eluded discovery, and it is only thanks to the greatly reduced brightness contrast in the mid-IR that it was found. In fact, the core of IRS1 is with an $N1$-band flux density of $N_{\mathrm{core}} = 0.573 \pm 0.029$ Jy (circular aperture of $2''$ diameter) nearly equally bright as σ Orionis, which has $N = 0.617 \pm 0.031$ Jy. The core of IRS1 is marginally resolved in the $N1$-band: its *FWHM* is $1.1''$, about 1.5 times greater than the *FWHM* of σ Orionis.

To estimate the contribution of the extended emission to the total integrated emission from IRS1, we also measured the brightness of IRS1 within a rectangular box of $4.4'' \times 3.2''$ (comparing with the brightness of the standard stars within an identical area), and found $N_{\mathrm{core+extended}} = 0.901 \pm 0.045$ Jy. The IRAS 12 μm flux density is $S_{12} = 4.5 \pm 0.2$ Jy[1], the $Q1$-band brightness of the core of IRS1 is $Q_{\mathrm{core}} = 2.38 \pm 0.24$ Jy, and the IRAS 25 μm flux density is $S_{25} = 15 \pm 2$ Jy.

3.2. Spectroscopy

N-band spectra were obtained *simultaneously* for σ Orionis and the core of σ Ori IRS1 (Fig. 2). The spectrum of σ Orionis follows the Rayleigh-Jeans tail of the photospheric emission of this hot star, $\lambda F_\lambda \propto \lambda^{-3}$. The spectrum of σ Ori IRS1, however, is dominated by a strong and broad emission feature, which we attribute to silicate dust. The silicate feature has weak shoulders at $\lambda \simeq 8.6$ and $11.7\,\mu$m and, although the spectral region

---

[1] The IRAS flux densities were redetermined from the original scans on the IRAS data server in Groningen.

between $\lambda = 9$ and 9.9 μm was useless due to a defunct channel in the TIMMI-2 array, it appears to peak around $\lambda \simeq 11$ to 11.3 μm. The underlying continuum is very red, with a flux ratio between $\lambda = 13$ and 8 μm of $F_{13}/F_8 \simeq 10$.

4. Analysis

4.1. Gas properties

The fan-shaped morphology of the extended mid-IR emission from σ Ori IRS1 suggests that it is acted upon by the intense radiation field of σ Orionis, either through radiation pressure on dust grains or through photo-evaporation of gas interspersed with the dust. The projected distance beween σ Ori IRS1 and σ Orionis is only $d \simeq 1200$ AU! The stellar wind of the main-sequence star σ Orionis, however, is too weak to have a significant impact.

The radio emission is consistent with optically thin free-free emission at wavelengths of $\lambda = 2$ and 6 cm, possibly becoming optically thick around a wavelength of $\lambda \simeq 15$ cm (Fig. 3). The latter can be used to estimate the electron density in the emission region (Osterbrock 1974): $\tau = 8.24 \times 10^{-2} \, T_e^{-1.35} \nu^{-2.1} \int n_+ n_e \mathrm{d}s$. For $\tau = 1$, with an electron temperature $T_e = 10\,000$ K, frequency $\nu = 2$ GHz and pathlength $\mathrm{d}s \simeq 10^{-3}$ pc, the electron density is estimated to be $n_e = n_+ \simeq 10^6$ cm^{-3}, which is indicative of a relatively dense, ionized region. The radio position (Drake 1990) is located 2.63″ North and 0.18″ East from σ Orionis, at the rim of the extended mid-IR emission facing σ Orionis. This suggests that the free-free emission arises from a photo-ionized region at the interface between the radiation field of σ Orionis and the dust region in σ Ori IRS1.

If the ionizing radiation from σ Orionis is absorbed in a layer with a thickness comparable to the radius r of the ionization front, then, following Bally & Reipurth (2001), the electron density is $n_e \simeq (L_H/4\pi\alpha_B r)^{\frac{1}{2}} d^{-1}$. With a Lyman continuum photon rate from σ Orionis of $L_H \simeq 10^{48}$ s^{-1} (Peimbert et al. 1975), recombination coefficient $\alpha_B = 2.6 \times 10^{-13}$ cm^3 s^{-1} (Osterbrock 1974), distance $d \simeq 1200$ AU from σ Orionis and size $r \simeq 300$ AU, we obtain $n_e \simeq 0.5 \times 10^6$ cm^{-3}. This is consistent with the value estimated from the radio emission, which implies that IRS1 cannot be much further away from σ Orionis than the projected $d \simeq 1200$ AU.

Photo-evaporation of the gas drives a mass-loss rate of $\dot{M}[M_\odot \, \mathrm{yr}^{-1}] \simeq 7.5 \times 10^{-6}(L_H/10^{49})^{\frac{1}{2}}(d/1 \, \mathrm{pc})^{-1}(r/0.1 \, \mathrm{pc})^{\frac{3}{2}}$ (Bally & Reipurth 2001), which for σ Ori IRS1 results in a mass-loss rate of $\dot{M} \simeq 7 \times 10^{-7} \, M_\odot \, \mathrm{yr}^{-1}$. If the estimated ion density of $n \simeq 10^6$ cm^{-3} is representative for a uniform gas density in a region of $r \simeq 300$ AU, then the total gas mass is of order $M_{gas} \sim 10^{-3} \, M_\odot$. The photo-evaporation timescale is thus much shorter than the age of σ Orionis. Therefore, there must be a reservoir of neutral material feeding the ionization front. As the radial density profile is expected to rise towards the centre of IRS1, the gas mass estimate should be regarded as a lower limit to the total amount of gas contained within the object.

The Hα surface brightness of the ionization front is $I[\mathrm{erg} \, \mathrm{s}^{-1} \, \mathrm{cm}^{-2} \, \mathrm{arcsec}^{-2}] \simeq 2.0 \times 10^{-18} n_e^2 (r/1\mathrm{pc})$ (Spitzer 1978),
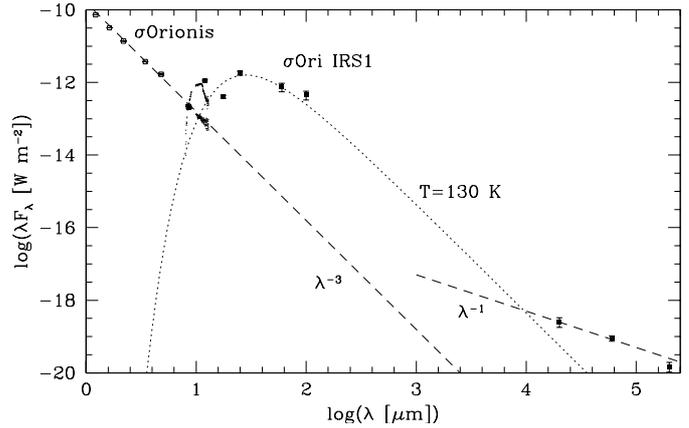

Fig. 3. Spectral energy distributions of σ Orionis, purely photospheric, and σ Ori IRS1, reproduced by a combination of thermal dust radiation ($T_{dust} = 130$ K) and free-free emission.

where we have assumed that the line-of-sight depth of the region is approximately r. We thus obtain $I \simeq 3 \times 10^{-9}$ erg s^{-1} cm^{-2} arcsec^{-2}. For σ Orionis, the flux density around Hα is $F \simeq 1.3 \times 10^{-9}$ erg s^{-1} cm^{-2} nm^{-1}. Through a narrow-band Hα filter with $\Delta\lambda$ of a few nm, the (surface) brightness of the ionized region in IRS1 would appear very similar to that of σ Orionis at a seeing of $\simeq 1''$, and at $>2''$ distance it would be easily resolved.

4.2. Dust properties

The IRAS position is $\sim 5''$ North and $\sim 12''$ East from σ Orionis, with an error ellipse of $18'' \times 5''$ under an angle of $87°$ from North to East. This is more consistent with the location of σ Ori IRS1 than σ Orionis. Indeed, whilst the spectral energy distribution of σ Orionis follows the Rayleigh-Jeans tail of its photospheric continuum emission, the continuum of the mid-IR spectrum and photometry of σ Ori IRS1 can be modelled by a Planck curve with a (dust) temperature of $T_{dust} = 130 \pm 10$ K (Fig. 3).

The structure in the dust emission feature of σ Ori IRS1 shows clear evidence for the dust to have been processed compared to interstellar dust. The latter is dominated by small amorphous silicate grains, with a typical radius of $a \simeq 0.1$ μm, of which the emission feature peaks sharply at $\lambda = 9.8$ μm and has a gradual downward slope towards $\lambda \sim 12$ μm. The observed feature in the spectrum of σ Ori IRS1 is much broader, and peaks at a significantly longer wavelength. Bouwman et al. (2001) show that the overall breath of the feature may be reproduced by larger grains, with a radius $a \simeq 1$ μm, that the peak at $\lambda \simeq 11.2$ μm indicates the presence of Mg-rich crystalline silicate (forsterite), and that the shoulder at $\lambda \simeq 8.6$ μm can be explained by silica (SiO_2). Such a mixture is often seen in environments in which the dust is expected to have been processed by co-agulation, leading to grain growth, and thermal annealing, producing crystalline grains and silica. Indeed, the spectrum of σ Ori IRS1 resembles that of β Pictoris and comet Hale-Bopp (Bouwman et al. 2001).

Letter to the Editor

An estimate of the total dust mass may be obtained by assuming that the dust emission is optically thin at mid-IR wavelengths. For an ensemble of N dust grains of radius a, at a distance $d_\oplus$ from Earth, the observed flux density is $F_\lambda = N(a/d_\oplus)^2 \pi B_\lambda$. The dust emission can be described by a Planck curve with a single dust temperature $T_{dust} = 130$ K, and it therefore does not matter at which wavelength we evaluate the flux density. At $\lambda = 25$ μm, $F_\lambda = 15$ Jy, and with $a = 1$ μm and $d_\oplus = 352$ pc we obtain $N \simeq 2 \times 10^{37}$ dust grains. At a typical density of $\rho = 2.5$ g cm^{-3}, this corresponds to a total dust mass of (only) $M_{dust} \sim 10^{-7}$ $M_\odot$. We note, however, that much more mass may be hidden in larger grains, rocks and planetesimals without being observable. From the estimated gas mass of $M_{gas} > 10^{-3}$ $M_\odot$, for a reasonable gas-to-dust mass ratio of order 10^2, a dust mass of $M_{dust} > 10^{-5}$ $M_\odot$ would be expected – which indeed suggests that most of the dust is locked up in larger pockets than the 1 μm grains that dominate the mid-IR radiation.

A certain fraction of the light from σ Orionis AB within a solid angle ω, subtended by IRS1 as seen from σ Orionis, is absorbed by the dust and re-radiated isotropically: $N4\pi a^2 \sigma T_{dust}^4 < (\omega/4\pi)L_\star$. With $L_\star \simeq 100\,000$ $L_\odot$, we obtain a solid angle of $\omega > 0.0013$ sterad. With a radius $R \simeq 300$ AU, this corresponds to an upper limit to the distance from σ Orionis of $d < 15\,000$ AU. This agrees with the morphology of IRS1, the location of the radio source, and the estimates for the electron density in the ionization front, which all suggest that we have a (roughly) side-view of the IRS1-σ Orionis couple, with a separation close to the projected distance of $d \simeq 1200$ AU.

5. The nature of σ Ori IRS1

The dust cloud σ Ori IRS1 measures $\sim 10^3$ AU across and contains $>10^{-3}$ $M_\odot$ of gas and dust, the latter of which shows signs of co-agulation. This suggests that IRS1 may be a proto-planetary disk. Indeed, circumstellar disks have been detected around several T Tauri stars in the σ Orionis cluster (Oliveira et al. 2003). As expected, the close proximity of IRS1 to σ Orionis gives rise to an ionization front at the side of IRS1 facing the O star, and it thus resembles the photo-evaporating proto-planetary disks seen in H II regions such as the Orion Nebula, otherwise known as "proplyds" (O'Dell et al. 1993). The rapid photo-destruction timescale is a problem though, unless the total mass contained within the disk of σ Ori IRS1 amounts to at least one solar mass or the object has been (much) further away during most of its past lifetime.

However, there is no evidence yet that σ Ori IRS1 hosts a central star. Hence the possibility remains that IRS1 is instead a dense knot of interstellar material – albeit processed – perhaps similar to the starless small clouds discovered recently in the Carina Nebula, a 3 Myr old massive star forming region (Smith et al. 2003). The proximity of IRS1 to σ Orionis may well be only temporary, alleviating the problem of the rapid photo-destruction. This would imply that such clouds must be rather common around σ Orionis, something which can be tested by means of a deep survey of the entire σ Orionis cluster at mid/far-IR or (sub)mm wavelengths.

References

Bally, J., & Reipurth, B. 2001, ApJ, 546, 299
Bouwman, J., Meeus, G., de Koter, A., et al. 2001, A&A, 375, 950
Brandner, W., Grebel, E. K., Chu, Y.-H., et al. 2000, AJ, 119, 292
Brown, A. G. A., de Geus, E. J., & de Zeeuw, P. T. 1994, A&A, 289, 101
Chlebowski, T., & Garmany, C. D. 1991, ApJ, 368, 241
Drake, S. A. 1990, AJ, 100, 572
Haisch, K. E., Lada, E. A., & Lada, C. J. 2001, ApJ, 553, L153
Heintz, W. D. 1997, ApJS, 111, 335
Hofmann, K.-H., Seggewiss, W., & Weigelt, G. 1995, A&A, 300, 403
Lucy, L. B. 1974, AJ, 79,745
McCaughrean, M. J., & Stauffer, J. R. 1994, AJ, 108, 1382
O'Dell, C. R., Wen, Z., & Hu, X. 1993, ApJ, 410, 696
Oliveira, J. M., Jeffries, R. D., Kenyon, M. J., Thompson, S. A., & Naylor, T. 2002, A&A, 382, L22
Oliveira, J. M., Jeffries, R. D., van Loon, J. Th., & Kenyon, M. J. 2003, in Open Issues of Local Star Formation and Early Stellar Evolution, ed. J. Gregorio-Hetem, & J. Lépine
Osterbrock, D. E. 1974, Astrophysics of Gaseous Nebulae (San Francisco: W.H. Freeman and Company), 79
Peimbert, M., Rayo, J. F., & Torres-Peimbert, S. 1975, Rev. Mex. Astron. Astrofis., 1, 289
Smith, N., Bally, J., & Morse, J. A. 2003, ApJ, 587, L105
Spitzer, L. 1978, Physical Processes in the InterMedium (New York: Wiley)
Walter, F. M., Wolk, S. J., & Sherry, W. 1997, in The 10th Cambridge Workshop on Cool Stars, Stellar Systems and the Sun, ed. R. A. Donahue, & J. A. Bookbinder, ASP Conf. Ser., 154, 1793
Zapatero Osorio, M. R., Béjar, V. J. S., Martín, E. L., et al. 2000, Science, 290, 103